AEDC-TR-67-3

AN EXPERIMENTAL INVESTIGATION OF FIXED-GEOMETRY DIFFUSERS IN AN OPEN-JET WIND TUNNEL AT MACH NUMBERS BETWEEN 14 AND 18 AND REYNOLDS NUMBERS BETWEEN 8,900 AND 25,000

James J. White, III

ARO, Inc.

March 1967

PROPULSION WIND TUNNEL FACILITY
ARNOLD ENGINEERING DEVELOPMENT CENTER
AIR FORCE SYSTEMS COMMAND
ARNOLD AIR FORCE STATION, TENNESSEE

NOTICES

When U. S. Government drawings specifications, or other data are used for any purpose other than a definitely related Government procurement operation, the Government thereby incurs no responsibility nor any obligation whatsoever, and the fact that the Government may have formulated, furnished, or in any way supplied the said drawings, specifications, or other data, is not to be regarded by implication or otherwise, or in any manner licensing the holder or any other person or corporation, or conveying any rights or permission to manufacture, use, or sell any patented invention that may in any way be related thereto.

Qualified users may obtain copies of this report from the Defense Documentation Center.

References to named commercial products in this report are not to be considered in any sense as an endorsement of the product by the United States Air Force or the Government.

AN EXPERIMENTAL INVESTIGATION OF FIXED-GEOMETRY DIFFUSERS IN AN OPEN-JET WIND TUNNEL AT MACH NUMBERS BETWEEN 14 AND 18 AND REYNOLDS NUMBERS BETWEEN 8,900 AND 25,000

James J. White, III
ARO, Inc.

AF - AEDC
Arnold AFS Tenn

FOREWORD

The work reported herein was performed at the request of Headquarters, Arnold Engineering Development Center (AEDC), Air Force Systems Command (AFSC), under Program Element 62410034, Project 7778, Task 777805.

The results presented were obtained by ARO, Inc. (a subsidiary of Sverdrup & Parcel and Associates, Inc.), contract operator of AEDC, AFSC, Arnold Air Force Station, Tennessee, under Contract AF40(600)-1200. The investigation was conducted during the period of August 1963 through June 1966, in the Propulsion Wind Tunnel Facility under ARO Project No. PL2290, and the manuscript was submitted for publication on December 20, 1966.

The author wishes to express his appreciation to Mr. J. C. Marshall, ARO, Inc., for his suggestions and assistance during this investigation.

This technical report has been reviewed and is approved.

William I. Kannawin
Major, USAF
Technology Division
Directorate of Plans and Technology

Edward R. Feicht
Colonel, USAF
Director of Plans and Technology

ABSTRACT

A fixed-geometry diffuser system was tested in an arc-heated, hypersonic, open-jet wind tunnel facility at Mach numbers between 14 and 18 and Reynolds numbers (based on nozzle exit diameter) between 8,900 and 25,000. Tests were conducted both with an empty test section and with conical models in the flow. Test variables included test section open-jet length, diffuser second-throat length, and diffuser inlet geometry. Diffuser efficiency improved with increased diffuser second-throat length, with increasing Reynolds number, and with the addition of conical models into the flow. Changes in open-jet length and diffuser inlet geometry had no appreciable effect on diffuser efficiency with an empty test section. A streamlined model support strut produced marked improvement in diffuser efficiency over a blunt support strut.

CONTENTS

TABLE

APPENDIXES

I. ILLUSTRATIONS

Figure

NOMENCLATURE

A	Area
A_{NE}	Nozzle exit area
A_{ST}	Diffuser second-throat area
D*	Nozzle throat diameter
D_{NE}	Nozzle exit diameter
D_{ST}	Diffuser second-throat diameter

L_j	Open-jet length measured from nozzle exit plane to diffuser inlet plane
L_{SSF}	Supersonic flow length measured from throat station of the nozzle to the end of the diffuser second-throat section
L_{ST}	Diffuser second-throat length
M_∞	Free-stream Mach number on the flow centerline
$\mathring{m}$	Mass flow
p_c	Test chamber pressure
p_d	Diffuser exit wall static pressure
p_{ST}	Static pressure at end of diffuser second throat
p_t	Stilling chamber pressure
p_t'	Test section impact pressure
p_t', d	Diffuser downstream impact pressure on the flow centerline
p_t', ST	Impact pressure at end of diffuser second throat on the flow centerline
p_t', ∞	Test section impact pressure on the flow centerline
Re_D	Test section Reynolds number, $\frac{\rho_\infty U_\infty D_{NE}}{\mu_\infty}$
T_t	Stilling chamber temperature
U	Velocity
U_∞	Free-stream velocity on the flow centerline
α	Momentum flux ratio at nozzle exit
β	Mass flux ratio at nozzle exit
η	Diffuser efficiency, $\frac{p_d}{p_t', \infty} \times 100$
μ_∞	Viscosity of the free-stream flow on the flow centerline
ρ	Density
ρ_∞	Free-stream density on the flow centerline

SECTION I
INTRODUCTION

One of the main problems in designing a low density, hypervelocity wind tunnel is the selection of a pumping system to handle the mass flows required at the very low pressures. Any available energy which can be recovered in the form of pressure will lessen the cost of a pumping system or, in an intermittent-type tunnel, increase the run time. The diffuser recovery pressure in a fixed-geometry diffuser system decreases with decreasing Reynolds number (Refs. 1 and 2). The present study was conducted as a part of the continuing wind tunnel research effort at AEDC to establish diffuser design information on low density testing facilities.

Tests were conducted in an arc-heated, open-jet wind tunnel facility with a fixed-geometry diffuser system. The tests were performed both with and without blockage models at Mach numbers between approximately 14 and 18 and at Reynolds numbers (based on nozzle-exit diameter) between 8,900 and 25,000. The test variables included diffuser second-throat length, open-jet length, diffuser inlet geometry, nozzle throat diameter (area ratio), and stilling chamber stagnation conditions.

SECTION II
APPARATUS

2.1 GENERAL DESCRIPTION

The experimental data were obtained in an 18-in. hypervelocity, low density, open-jet wind tunnel. The tunnel is powered by a 250-kw d-c electric arc heater which is operated with air as a test fluid. The heated air exhausts into a stilling chamber and is thence expanded through a nozzle into an open-jet test section. The test gas is collected and decelerated in a diffuser and exhausted by means of a six-stage steam ejector. A photograph of the facility is shown in Fig. 1 (Appendix I), and a schematic of the major components is exhibited in Fig. 2. A cutaway view of the test chamber showing the nozzle and initial portion of the diffuser is given in Fig. 3.

The arc heater consists of two water-cooled, electrically isolated, coaxial electrodes separated by a cylindrical vortex tube. The rear electrode acts as the anode, and the front electrode serves as the cathode and is the exit for the hot test gas. An auxiliary magnetic field coil serves

to rotate the arc in the anode to lessen electrode erosion and permit more uniform heating of the gas. Air inlet ports in the cylindrical vortex tube can be adjusted to vary the airflow pattern within the arc chamber.

The stilling chamber is the connecting link between the arc heater and nozzle. The chamber is 1.50 in. in diameter by 3.25 in. long and serves to improve the uniformity of the flow in the test section. The stilling chamber is water cooled.

The expansion section consists of a 10-deg half-angle conical nozzle which is water cooled over approximately half its length. Replaceable throat sections permit varying the throat diameter. The nozzle exit diameter is 18 in., and the minimum diameters of the two throat sections used in this test were 0.137 and 0.200 in.

The diffuser consists of an inlet section, a constant-diameter second-throat section, and a subsonic expansion section. The determination of the sizes for these various diffuser sections was made from the best information available at the time the tunnel was designed. Four diffuser inlet geometries were tested, and these are shown in Fig. 4. A photograph of the inlets is shown in Fig. 5. The inlets are mounted to the constant-diameter section by means of a slip joint and clamp. The open-jet length could be varied from two to one-half nozzle exit diameters by adding spacers at the slip joint. The second-throat section is 17.5 in. in diameter and consists of a 44.5-in.-long fixed portion and four removable sections which allow varying the second-throat length from 44.5 to 242.5 in. in 18-in. increments. When spacers are added to alter the open-jet length, the second-throat length could be additionally increased by as much as 27 in. With changes in inlet geometry, the second-throat length could further be increased by 18 in. A 3-deg half-angle subsonic diffusion section, which expands to 36.75 in. in diameter and terminates at the heat exchanger, completes the diffuser system. A photograph of the exterior portion of the diffuser is shown in Fig. 6. Pertinent diffuser system dimensions are given in Fig. 7. The diffuser system is not water cooled, and tunnel run times were limited to approximately 30 min because of diffuser heating.

A six-stage steam ejector supplies the pumping capability for the tunnel. This ejector has a design-point flow capability of 5 lb/hr with an inlet pressure of 0.007 torr and a maximum capacity of 280 lb/hr at pressures above 0.5 torr. A butterfly valve is installed between two ejector stages to regulate back pressure on the diffuser.

2.2 BLOCKAGE MODELS

The five blockage models used in this test were uncooled, 30-deg half-angle, blunted cones with a spherical nose radius of 0.25 in. Model base diameters ranged from 2 to 4 in. in 0.5-in. increments. The 4-in. conical model represents approximately a 25-percent test core blockage at the test condition for which blockage effects were assessed. A photograph of the models is shown in Fig. 8. The models were mounted in the test section by means of a water-cooled, swept support strut which was designed to give a minimum wake blockage and cell pressure rise. The strut is swept backward at a 30-deg angle and has a sharp single wedge profile with a 30-deg total wedge angle on the leading edge. The chord length perpendicular to the leading edge is 1.62 in. A photograph of one of the models on the swept support strut is shown in Fig. 9. A blunt support strut was also used to evaluate the effect of model support configuration on diffuser performance. This strut consists of a 1-in.-diam tube mounted perpendicular to the airstream and is pictured in Fig. 10. Both support struts were mounted onto a mechanism which allowed insertion of the model into the flow stream after flow was established.

2.3 IMPACT PRESSURE PROBES

Water-cooled impact probes were mounted in the test section, at the end of the diffuser second-throat section, and at the end of the diffuser expansion section. The test section probe has a conical tip with a 1/8-in.-diam, sharp-lipped inlet, a 0.75-in. outside diameter, and is mounted on a traversing mechanism which allows probe movement in both the transverse and axial directions. A photograph of the probe is shown in Fig. 11. Both downstream probes have a 0.200-in.-diam orifice on a 0.5-in.-diam flat face.

2.4 INSTRUMENTATION

2.4.1 System Instrumentation

The total enthalpy in the airstream was determined from a heat balance across the arc heater and stilling chamber. Power input to the arc heater was determined from measurements of the current and voltage, which were recorded continuously on a strip-chart recorder. Energy losses were assessed from measurements of water temperature rise across the cooled components by ten-element thermopiles and from associated water flow rates measured by turbine-type flowmeters. The enthalpy was also calculated using real-gas flow relationships through a choked nozzle. The heat balance method for calculating enthalpy was used in the reduction of the data.

However, the differences in the two calculations were included in the evaluation of data precision as quoted in Section 2.4.2.

A sharp-edged orifice was used in the high pressure air supply line to determine the mass flow rate. The pressure upstream of the orifice and the differential pressure across the orifice were measured with diaphragm-type, strain-gage pressure transducers. An associated air temperature measurement was made with an unshielded thermocouple. The stagnation pressure in the stilling chamber was also measured with a diaphragm-type, strain-gage pressure transducer.

Impact and static pressures were measured in the test chamber and along the diffuser. These pressures were measured with diaphragm-type, variable-capacitance pressure transducers designed to give good accuracy and installed to give rapid response at low absolute pressures. Locations of pressure measurements in the test chamber and diffuser are shown in Fig. 12.

2.4.2 Precision of Measurements

Calibrations were made periodically during this investigation on all instrumentation components and their associated recorders. The repeatability of all instrumentation components from one calibration to the next was excellent; however, any small deviations were taken into account in reducing the data.

The precision of measurement of the data presented in this report is given below:

η	p_t	p_c	p_d	T_t
±1	±0.35 atm	$\pm 5 \times 10^{-4}$ torr	$\pm 2.0 \times 10^{-2}$ torr	±300°K

These estimates were calculated by a statistical analysis method described in Ref. 3. All factors known to influence the measurements, and which could be assessed, are included in the calculations. The precisions quoted correspond to a confidence level of 95 percent.

SECTION III
EXPERIMENTAL PROCEDURE

3.1 TUNNEL OPERATION

The following procedure was used to obtain diffuser recovery data. The instrumentation and arc heater were checked out before tunnel

pumpdown. The entire tunnel was evacuated to a pressure from 0.01 to 0.02 torr. Reference zeroes were then taken on the pressure instrumentation in the test chamber and diffuser. High pressure demineralized water flow was initiated to the cooled components, and the airflow rate was adjusted for startup. The tunnel pressure ratio, p_t/p_d, was set to a value known to be in excess of the diffuser starting pressure ratio. The arc heater was started, and the airflow rate was then adjusted to obtain the desired stilling chamber pressure. If the run was made without a model, a centerline impact pressure measurement was taken 0.25 in. downstream of the nozzle exit plane, and then the impact probe was removed from the flow. If a model was to be tested, it was introduced into the flow on the tunnel centerline with the nose 0.25 in. downstream of the nozzle exit plane. (When testing with models, a centerline impact pressure was approximated by choosing an impact pressure from a tunnel-empty run for which the stagnation conditions closely approximated those for the individual model test run.) The tunnel pressure ratio was then decreased in small increments by closing the diffuser butterfly valve until the test chamber pressure began to change with changes in diffuser exit pressure. The process was continued until the test chamber pressure was approximately an order of magnitude higher than the original value. The tunnel pressure ratio was then increased in small increments until the diffuser flow was again started. A second impact pressure reading was then taken. At the end of a run, reference zeroes were taken on all recording instrumentation.

A sample of the data taken by the preceding method is given in Fig. 13. The three sets of data presented correspond to different nozzle area ratios and stilling chamber pressures and were taken at a tunnel-empty condition.

3.2 DATA REDUCTION

3.2.1 Test Section Flow Properties

The test section flow properties listed in Fig. 14 were calculated by assuming equilibrium flow from the stilling chamber to the nozzle throat and completely frozen (both vibrationally and chemically) flow from the throat to the test section. The justification for using this particular flow model was based on comparisons of test section flow properties determined by this flow model and by nonequilibrium flow calculations utilizing a high-speed digital computer (Ref. 4). Both chemical species concentrations and bulk thermodynamic properties were compared, and the differences were found to be small. With the flow model specified, free-stream flow properties were calculated as a function of Mach number through the

supersonic expansion portion of the nozzle. This calculation was continued for increasing Mach number until the calculated value of impact pressure ($p_t'_{,\infty} \approx \rho_\infty u_\infty^2$) was equal to the measured value of impact pressure on the centerline of the test section.

The variation of flow properties across the test section flow stream is represented by the impact pressure profiles given in Fig. 14. These profiles were taken at the nozzle-exit station.

3.2.2 Diffuser Efficiency

The diffuser efficiency used in presenting these results is

$$\eta = \frac{\text{Diffuser Exit Static Pressure}}{\text{Normal Shock Recovery Pressure on the Centerline}} \times 100$$

Since the boundary layer occupies a large portion of the flow field (boundary-layer thicknesses can be inferred from the impact pressure profiles in Fig. 14), the impact pressure on the nozzle centerline does not represent the average momentum in the flow field, and thus efficiencies of 100 percent would not be generally anticipated. However, since this form of expression for diffuser efficiency is widely used in presenting high Mach number facility performance results, it has been used herein to permit direct comparison with other data by the reader.

The normal shock recovery pressure on the nozzle centerline was measured with a sharp-lipped probe located 0.25 in. downstream of the nozzle exit. An impact pressure and a static pressure were measured at the diffuser exit. When the diffuser second throat was long, the diffuser exit static and impact pressures were nearly equal. With a short second-throat length, the centerline impact pressure was much higher than the static pressure. However, from partial impact pressure surveys taken across the diffuser exit, the static pressure and average impact pressure were still very nearly the same. Hence, the diffuser exit static pressure was used to represent the recovery of the diffuser. Differences between the static pressure and average impact pressure were included in the overall level of precision quoted for diffuser efficiency.

An equation for predicting the optimum diffuser recovery pressure in a hypersonic tunnel is

$$p_d \equiv \frac{\dot{m}\, U_\infty}{A_{ST}}$$

This equation represents the recovery pressure attainable if all the available momentum in the test section flow is converted into pressure. The derivation of this equation is given in Appendix II. Since the mass flow

rate and free-stream velocity are specified by the stilling chamber pressure, the air total enthalpy, and the nozzle throat diameter, the only way indicated to improve the diffuser recovery is to reduce the second-throat area. This assumes that the diffuser is sufficiently long to allow the momentum conversion process to be completed (see assumption (2), Appendix II). The required lengths must be determined experimentally. Other experimenters (e.g., Ref. 2) have shown this dependence of diffuser recovery on second-throat area. For the present tests, a diffuser area approximately equal to the nozzle-exit area was selected as a compromise between the desire for high recovery and the need to operate with relatively large and blunt models. The results presented in Section 4.2 would seem to substantiate this choice as a reasonable one.

SECTION IV
RESULTS AND DISCUSSION

Diffuser efficiencies are presented for tunnel operation with an empty test section and also with conical models present in the flow. Unless otherwise stated, the diffuser pressure used for defining the efficiency is obtained during the diffuser flow breakdown process (decreasing pressure ratio). Referring to Fig. 13, the diffuser pressure at flow breakdown is defined as the pressure which exists at the diffuser exit station when the test chamber pressure has risen 10 percent above its original value. The diffuser pressure used for defining the starting efficiency, which is given in several figures, is obtained while increasing the pressure ratio (see Fig. 13). The diffuser pressure when the flow has restarted is defined as the pressure which exists when the test chamber pressure is within 10 percent of its minimum value. Test variables include stagnation conditions, nozzle throat diameter, diffuser inlet geometry, test section open-jet length, and diffuser second-throat length. The effects of a streamlined and a blunt model support strut on diffuser efficiency are also compared.

4.1 EMPTY TEST SECTION

The effect of varying the test section open-jet length is given in Fig. 15 for four different flow conditions and two diffuser inlets. These data indicate that changes in open-jet length have no appreciable effect on diffuser recovery for the range of conditions covered. It should be noted that changes in open-jet length were produced by changing spacers to the second-throat duct and thus altered the length of the second throat (increasing L_j/D_{NE} resulted in a corresponding decrease in L_{ST}) but did not change the overall supersonic flow length (L_{SSF}).

Figure 16 demonstrates the effect of diffuser second-throat length on diffuser efficiency. It can be seen that diffuser efficiency increases with increased second-throat length and also increases with higher Reynolds number. Also shown in Fig. 16 is the calculated value of the optimum diffuser recovery obtained from the equations given in Section 3.2.2. By linear extrapolation of the diffuser efficiency curves to the optimum recovery, it can be observed that the diffuser second-throat length required to achieve optimum recovery would need to be greater for lower Reynolds numbers, provided near-optimum recovery can be obtained at all conditions.

Impact and static pressures were obtained at the end of the diffuser second throat. Referring to Fig. 17, it can be seen that the ratio of impact to static pressure, $p_{t',ST}/p_{ST}$, decreases with increasing second-throat length. Ideally, sonic flow would exist at the end of the second throat, and the pressure ratio would be approximately two. It appears that this condition could be achieved with an increased second-throat length, which has also been shown in the previous paragraph to be a necessary condition for achieving the optimum recovery.

The effect of diffuser inlet geometry on diffuser recovery was evaluated by testing the four diffuser inlets shown in Fig. 4. As can be seen in the following table, the diffuser efficiency was essentially the same for all of the inlets.

Even though all four inlets in this investigation produced test pressures below the nozzle exit static pressure, inlet No. 3 (which had the steepest inlet angle) produced slightly higher test chamber pressures at all conditions except the lower pressure with the smaller nozzle throat. This suggests that inlet angles less than 15 deg should be used to maintain high diffuser pumping effectiveness, and thus low test chamber pressures.

The starting characteristic of the diffuser after flow breakdown is shown in Fig. 13. At the low Reynolds numbers, the starting and breakdown pressure ratios are identical. However, it can be seen that as the Reynolds number increases, a hysteresis effect occurs, and the starting pressure ratio is greater than the breakdown pressure ratio.

4.2 MODEL BLOCKAGE

The effects of model blockage on diffuser performance were determined for one set of stagnation conditions. The effects of altering diffuser inlet geometry were not assessed.

TABLE I

EXPERIMENTAL DATA ON DIFFUSER INLET PERFORMANCE

INLET NO.	p_t, atm	D^*, in.	p_c, torr	η	L_j/D_{NE}
1	10	0.200	0.0126	21.7	1.5
2	↓	↓	0.0125	26.1	↓
3	↓	↓	0.0142	26.3	↓
4	↓	↓	0.0115	26.1	↓
1	20	0.200	0.0193	48.1	1.5
2	↓	↓	0.0175	46.6	↓
3	↓	↓	0.0250	46.1	↓
4	↓	↓	0.0190	44.4	↓
1	7	0.137	0.0070	11.7	1.5
2	↓	↓	0.0066	11.5	↓
3	↓	↓	0 0073	10.7	↓
4	↓	↓	0.0075	11.9	↓
1	≈ 10	0.137	0.0075	14.0	1.5
2	↓	↓	0.0075	14.6	↓
3	↓	↓	0.0090	14.6	↓
4	↓	↓	0.0083	15.0	↓

As shown in Fig. 18, changes in open-jet length produced varied results for the models tested. By comparing the results with those of Fig. 15, it is seen that the diffuser efficiency for various open-jet lengths is increased with models in the flow with the exception of the 4-in. conical model at the longest open-jet length ($L_j/D_{NE} = 2$).

The effect of changing diffuser second-throat length with models present in the flow parallels the tunnel-empty case; i.e., the diffuser efficiency increases continuously with increased second-throat length. From Fig. 19, it can be seen that diffuser efficiency is significantly increased with the models present in the flow, and thus the efficiency should reach the calculated optimum recovery value at a shorter second-throat length. By extrapolation of the top curve of Fig. 19, a diffuser length-to-diameter ratio of 16.25 would provide optimum diffuser recovery for the 2-in.-diam model at this test condition.

The diffuser would start with the 2-, 2.5-, and 3-in. conical models in the flow. Starting efficiencies for the 2- and 3-in. models are given in Fig. 20. The 3.5- and 4-in. models would not start with any of the second-throat lengths tested, although the flow would not break down when the models were inserted into the flow stream.

Figure 21 demonstrates the effect of the type of support strut used to hold the model. The diffuser efficiency with the streamlined support strut (Fig. 9) is more than double that for the blunt strut (Fig. 10) except for the shortest second-throat length. The increased efficiency with the streamlined strut is probably caused by a decreased wake blockage and a more efficient oblique shock system generated in the diffuser.

SECTION V
CONCLUSIONS

As a result of this experimental investigation, the following conclusions can be reached:

1. Changes in open-jet length for L_j/D_{NE} from 0.5 to 2 did not alter the diffuser efficiency for tests without models.
2. Diffuser efficiency improved with increased second-throat length both with and without models in the flow.
3. For the one set of stagnation conditions at which model data were obtained, higher diffuser recoveries were obtained when models were in the flow than for the tunnel-empty case.
4. Changing diffuser inlet geometry had an insignificant effect on diffuser recovery for tests with the tunnel empty.
5. Diffuser efficiency increased with increasing Reynolds numbers.
6. For optimum diffuser recovery, the indicated diffuser second-throat length increases with decreasing Reynolds numbers.
7. Using a streamlined model support strut resulted in diffuser efficiencies more than double those obtained using a blunt model support strut.

REFERENCES

1. Boylan, David E. "An Experimental Study of Diffusers in an Open-Jet, Low-Density, Hypersonic Wind Tunnel." AEDC-TDR-64-47 (AD434380), April 1964.

2. Clark, Lewis E. "Description and Initial Calibration of the Langley 12-Inch Hypersonic Ceramic-Heated Tunnel." NASA TN D-2703, March 1965.

3. Dean, Robert C., Jr. Aerodynamic Measurements. Gas Turbine Laboratory, Massachusetts Institute of Technology, Eagle Enterprises, Boston, 1953.

4. Marshall, John C., ARO, Inc. Private Communication. 1966.

APPENDIXES

I. ILLUSTRATIONS
II. DERIVATION OF THE EXPRESSION FOR THE OPTIMUM DIFFUSER RECOVERY PRESSURE

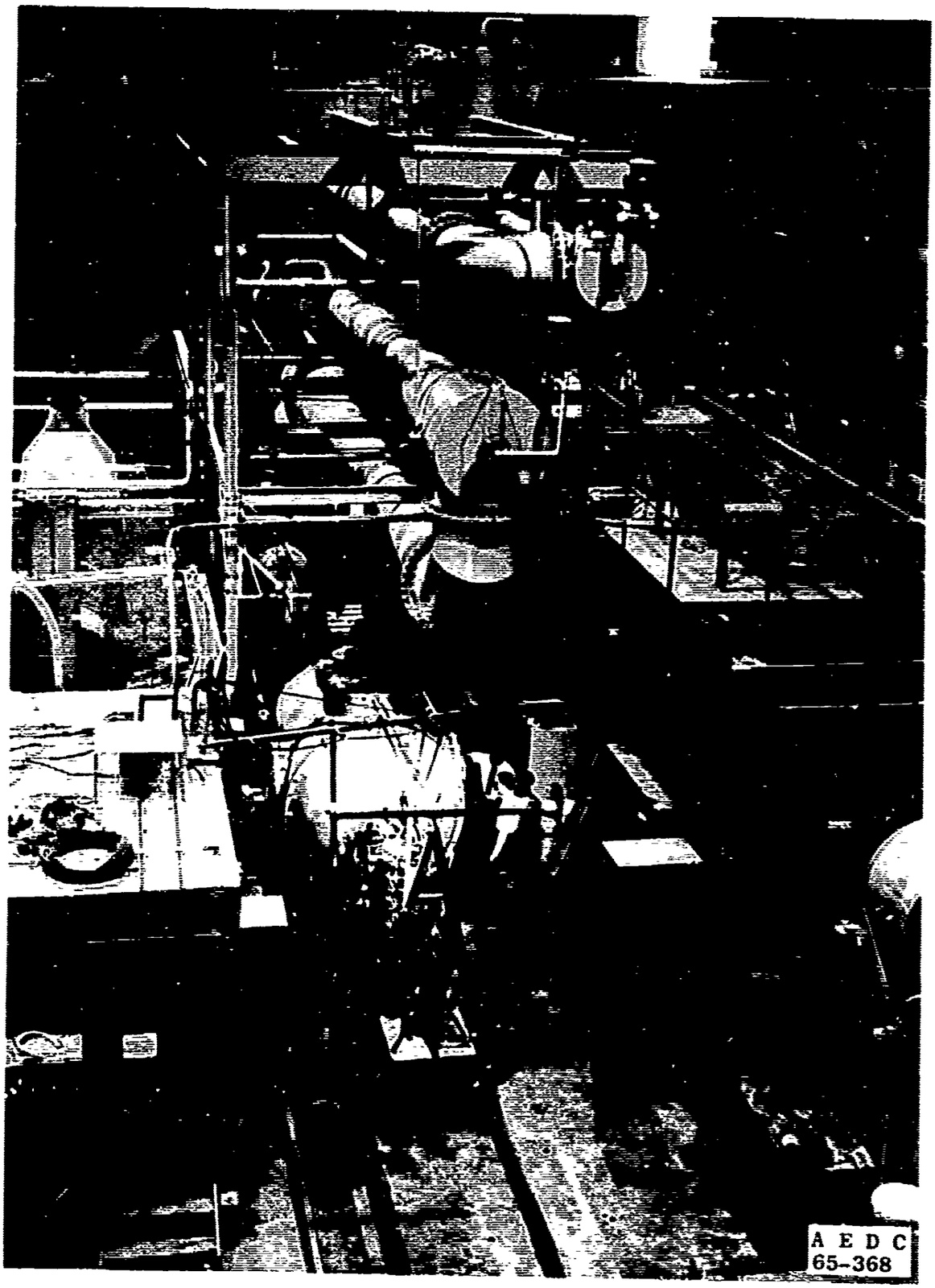

Fig. 1 The 18-in. Hypersonic Wind Tunnel

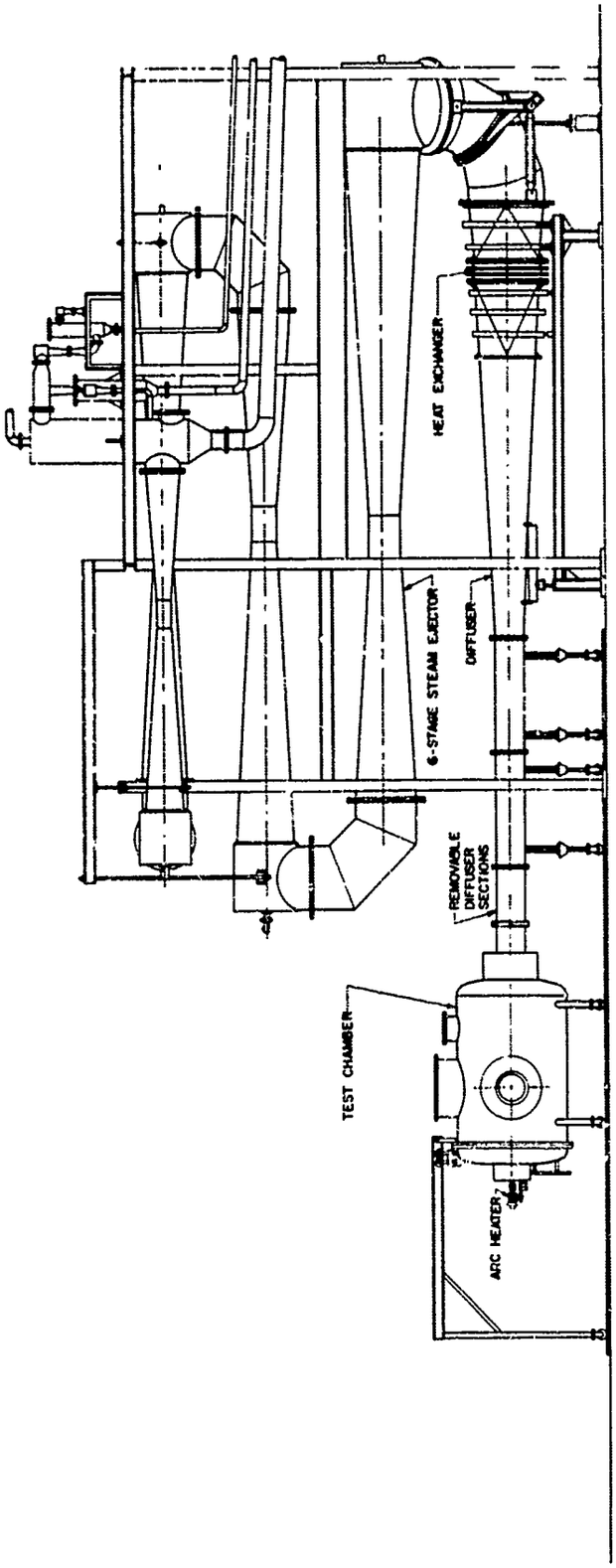

Fig. 2 Sketch of the 18-in. Hypersonic Wind Tunnel

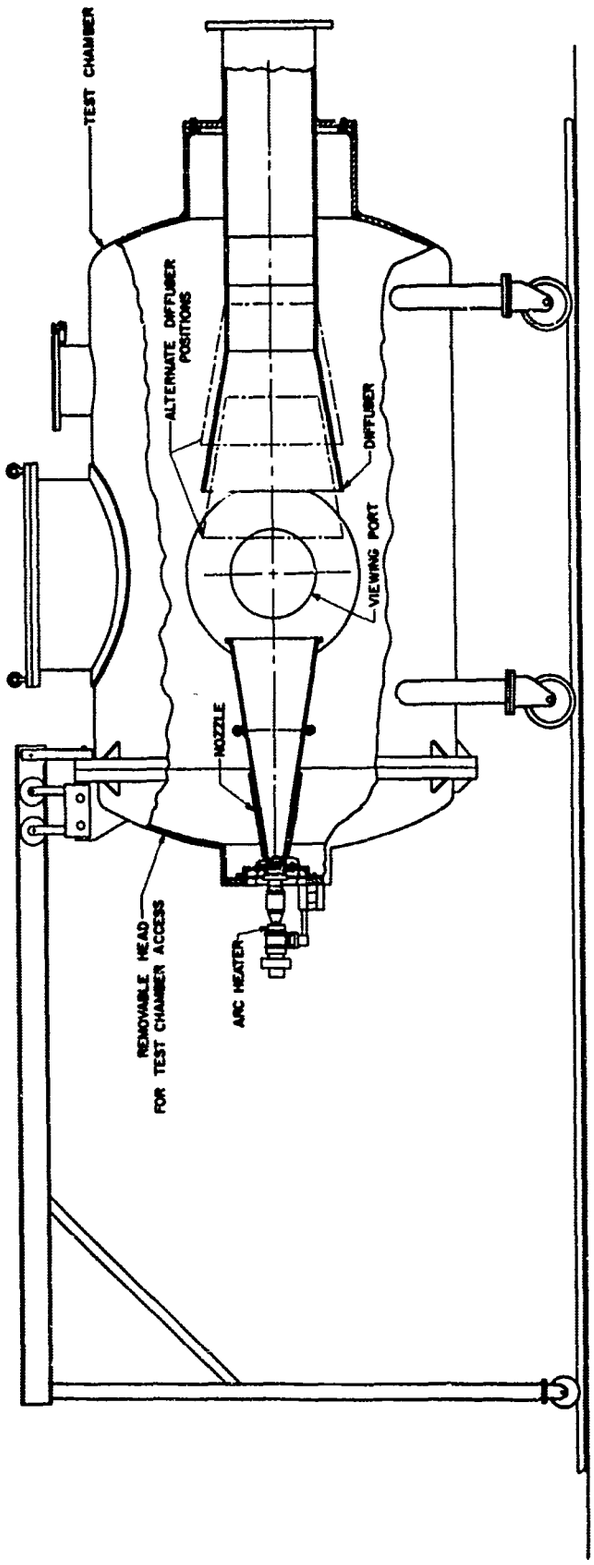

Fig. 3 Arrangement of Components in the Test Chamber

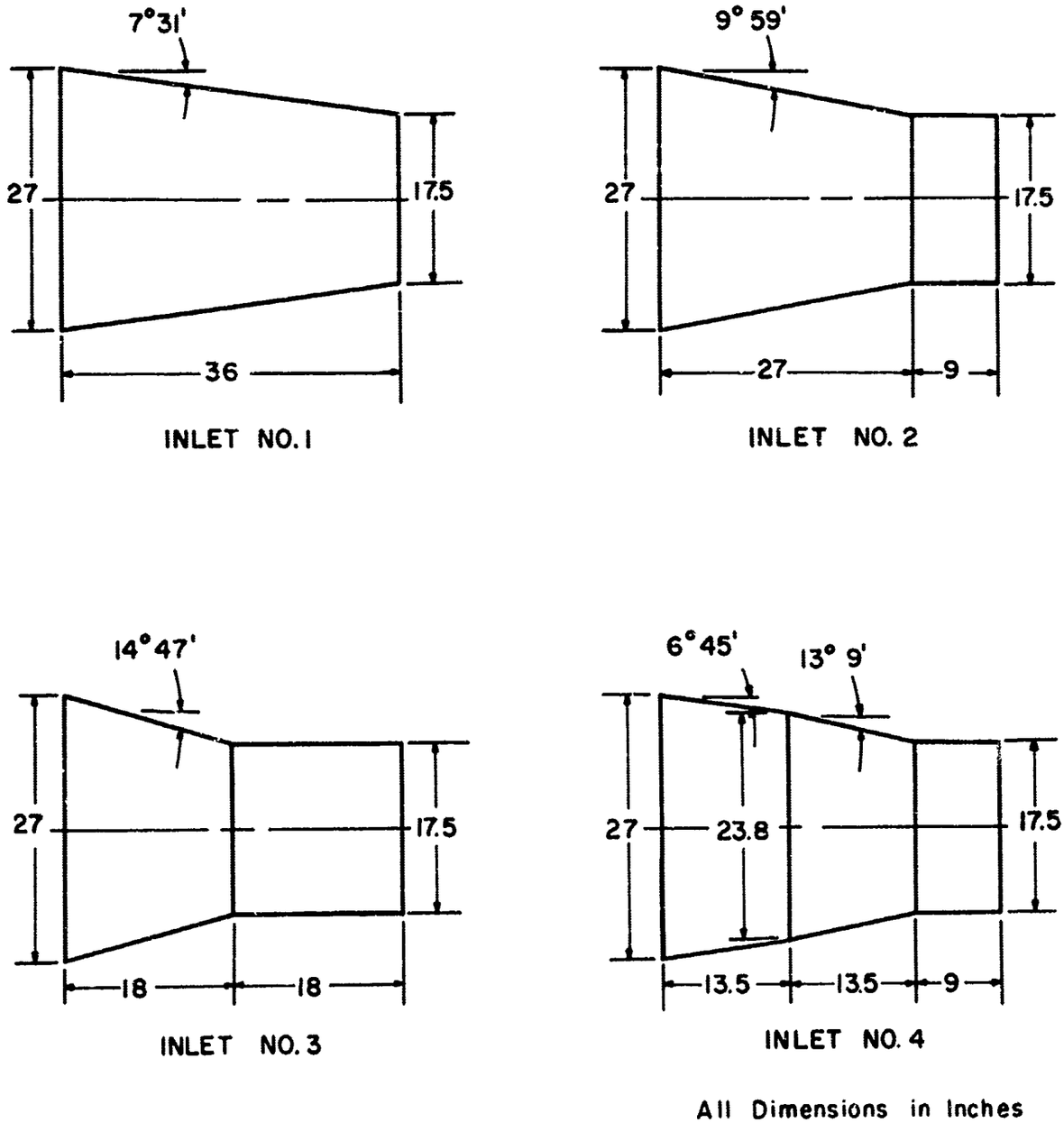

Fig. 4 Diffuser Inlet Geometries

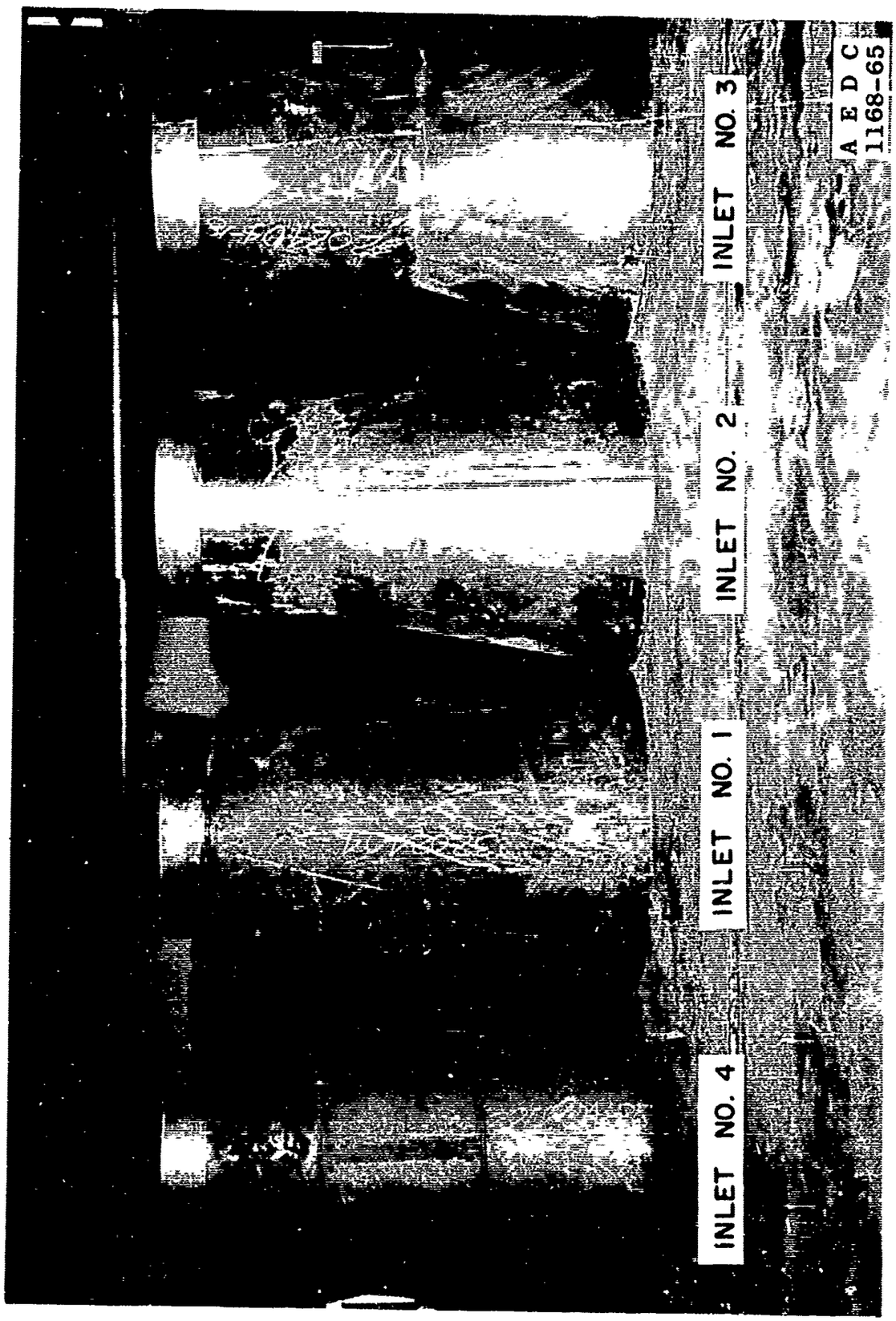

Fig. 5 Diffuser Inlets

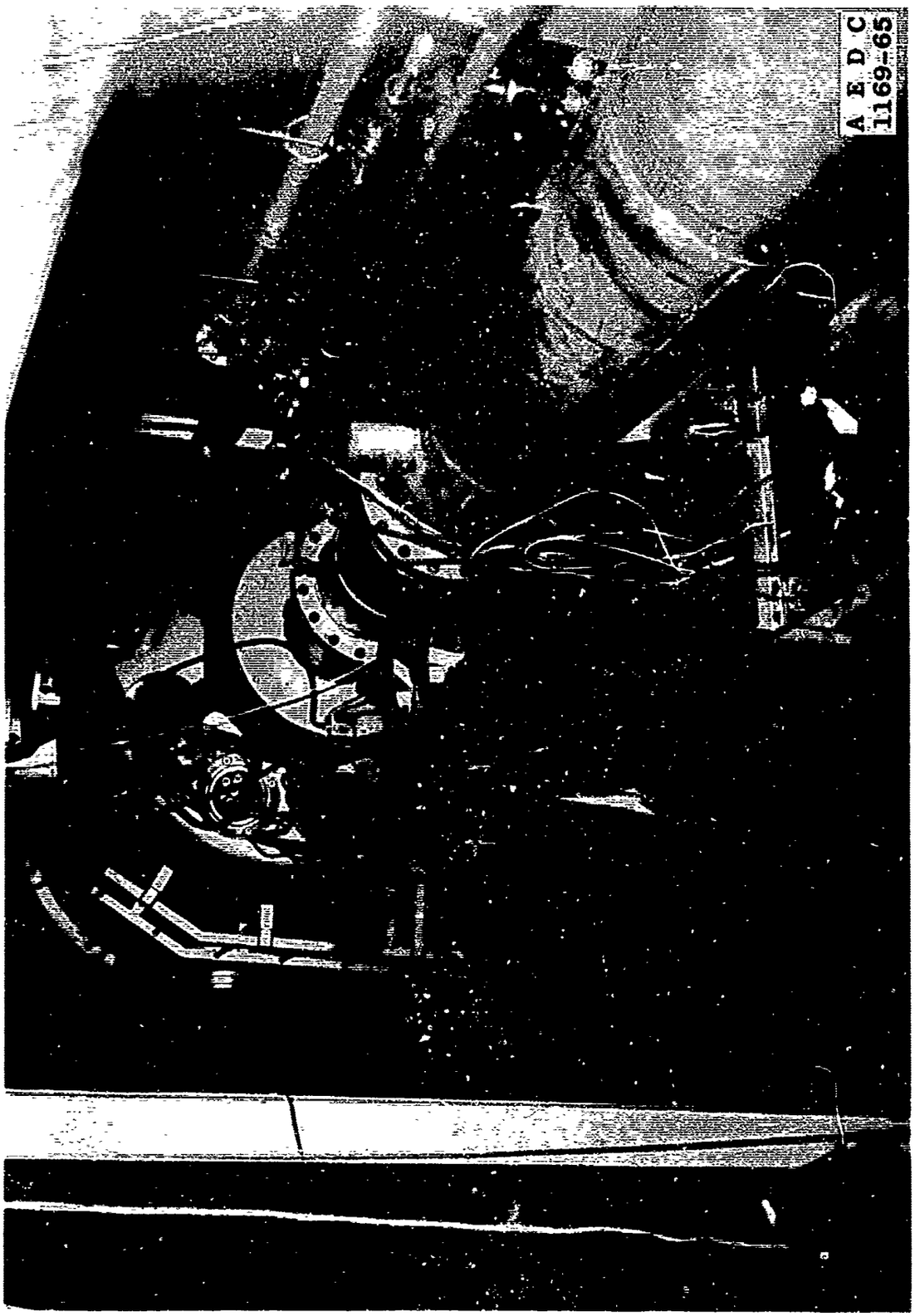

Fig. 6 Diffuser Exterior

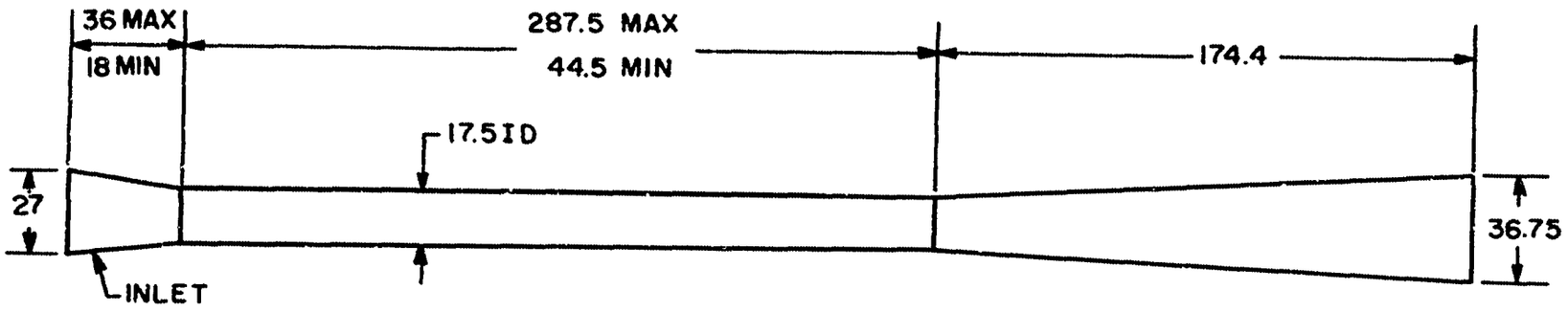

All Dimensions in Inches

Fig. 7 Diffuser Dimensions

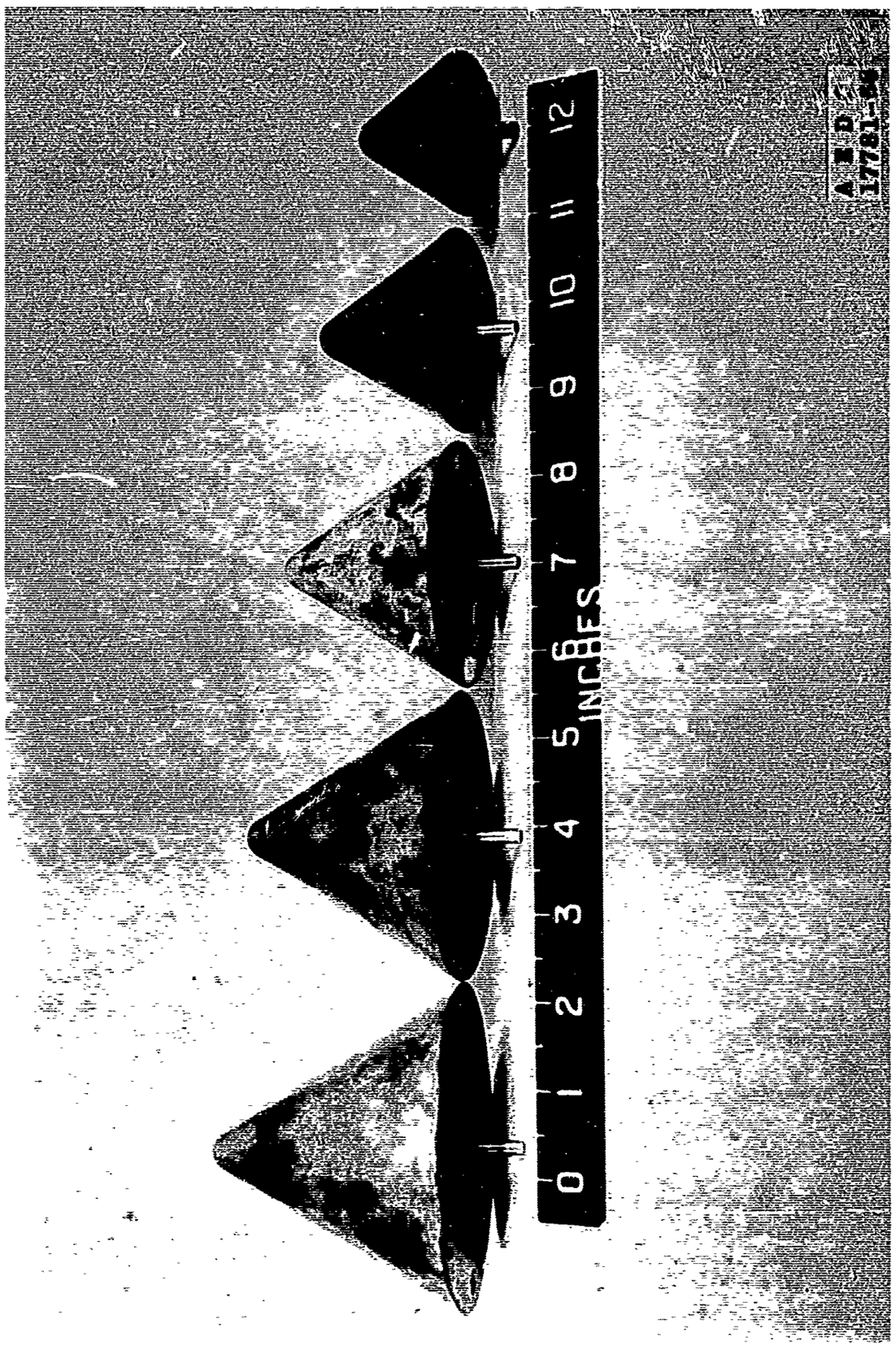

Fig. 8 Blockage Models

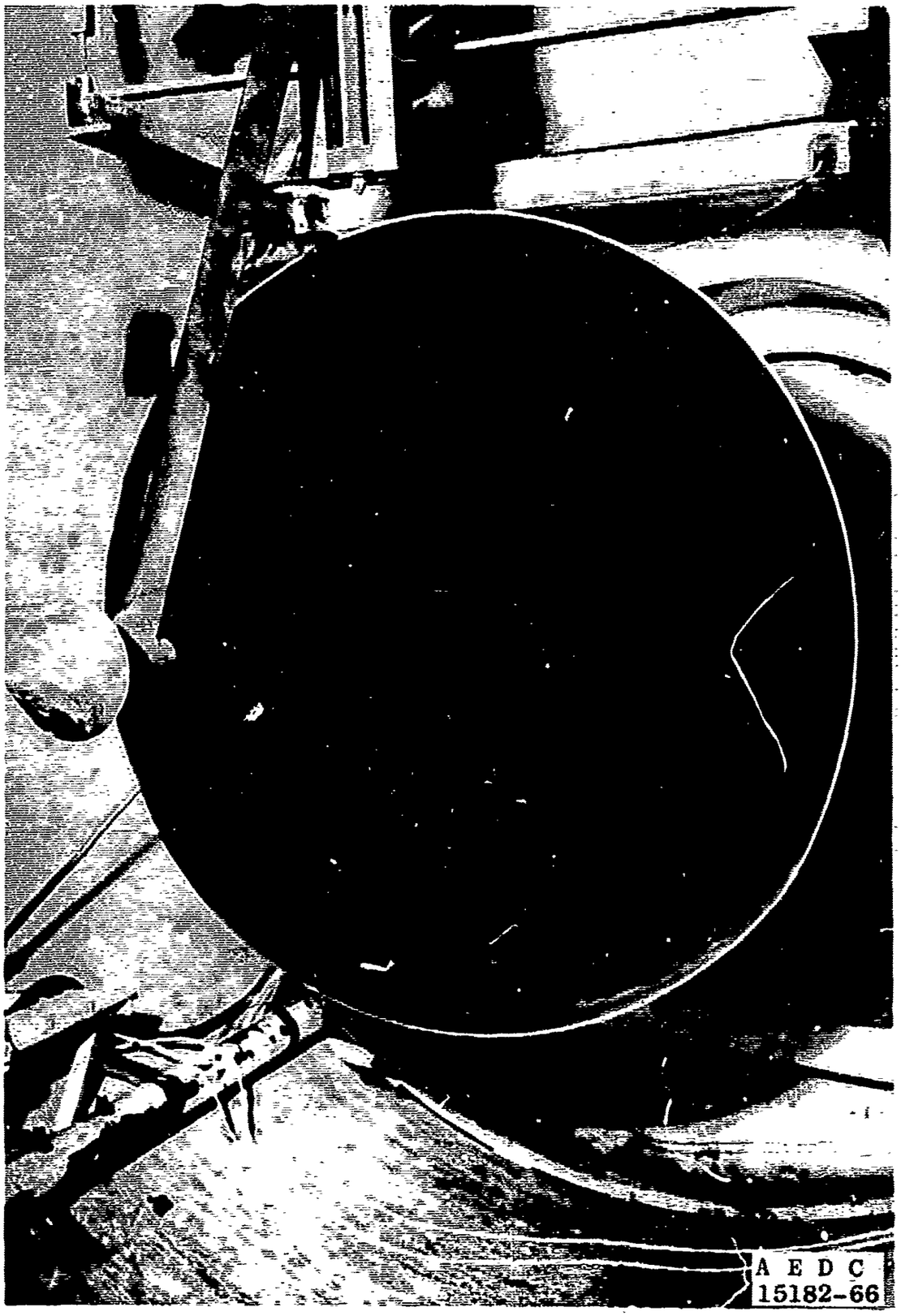

Fig. 9 Streamlined Model Support

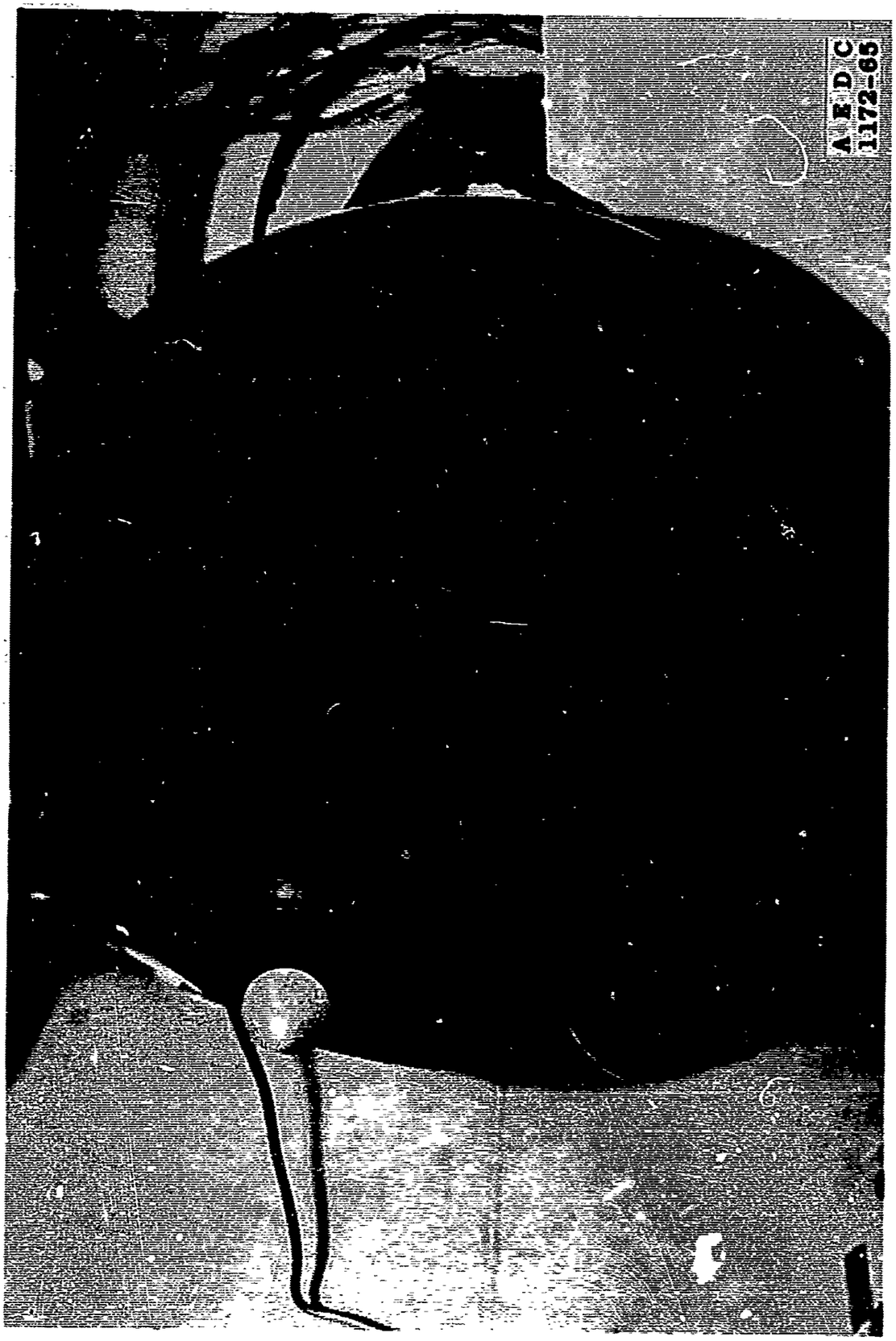

Fig. 10 Blunt Model Support

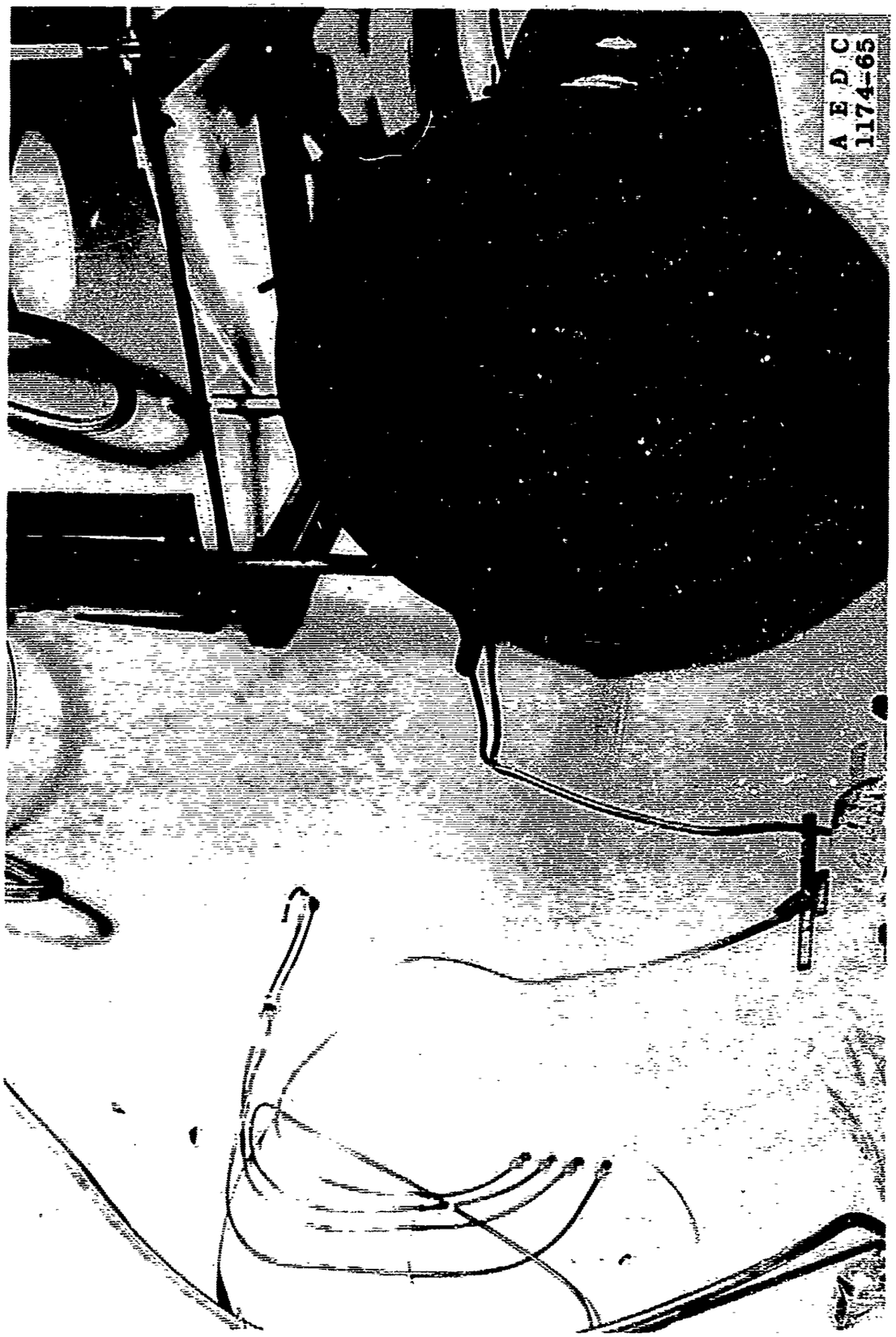

Fig. 11 Test Section Impact Pressure Probe

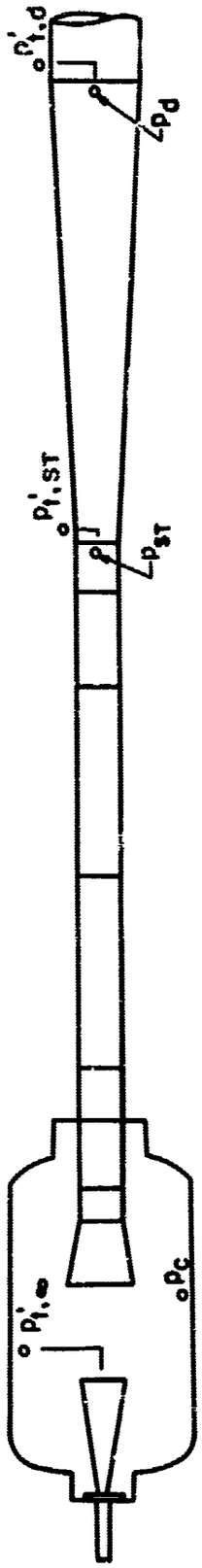

Fig. 12 Instrumentation Locations for Test Chamber and Diffuser

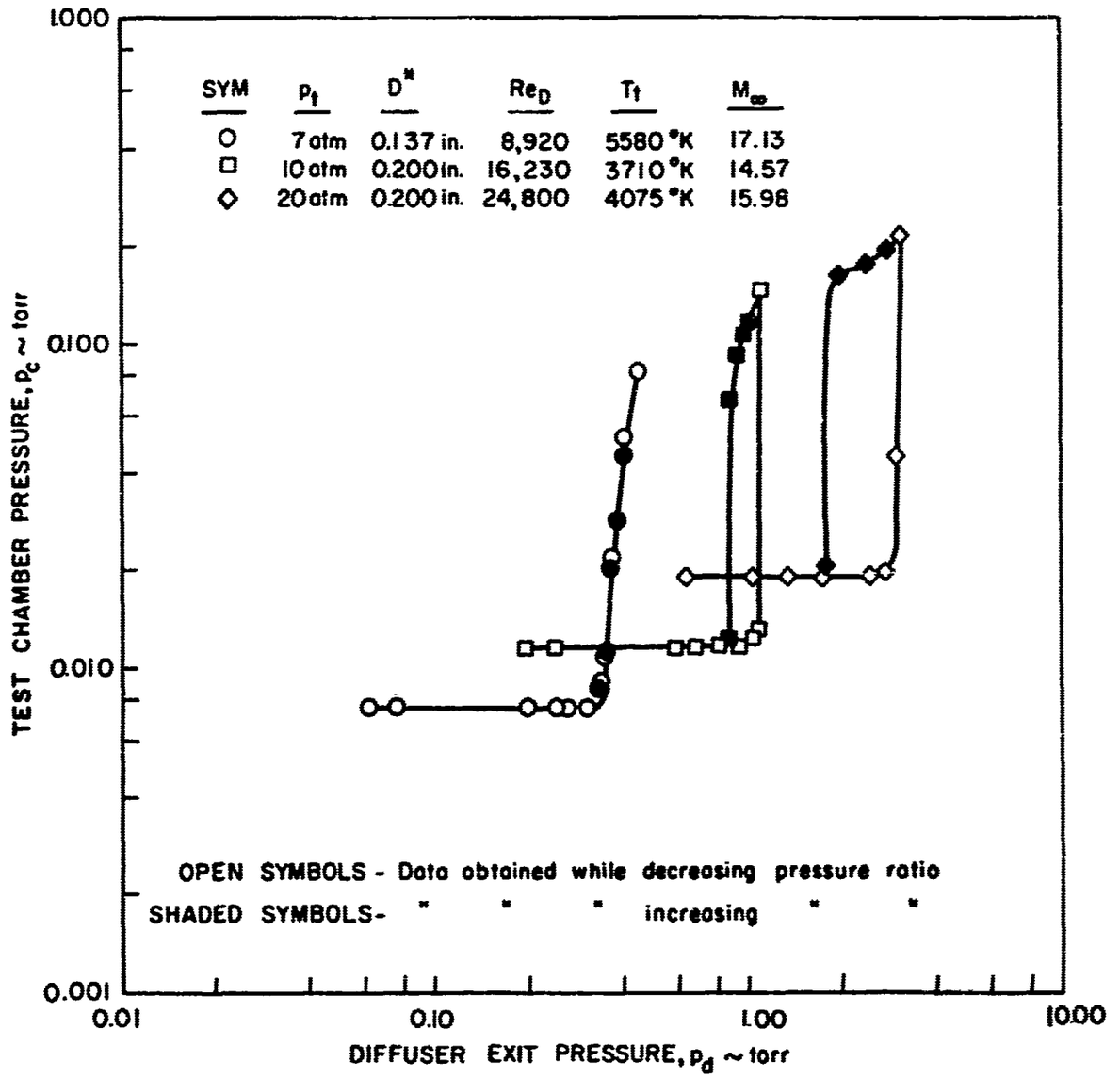

Fig. 13 Variation of Test Chamber Pressure with Diffuser Exit Pressure – Empty Test Section

SYMBOL	p_t	T_t	D^*	U_∞	M_∞	Re_D
○	7 atm	5580 °K	0.137 in.	11,872 ft/sec	17.13	8,920
△	10 atm	4660 °K	0.137 in.	10,663 ft/sec	17.26	11,970
□	10 atm	3710 °K	0.200 in.	9,298 ft/sec	14.57	16,230
◇	20 atm	4075 °K	0.200 in.	9,811 ft/sec	15.98	24,800

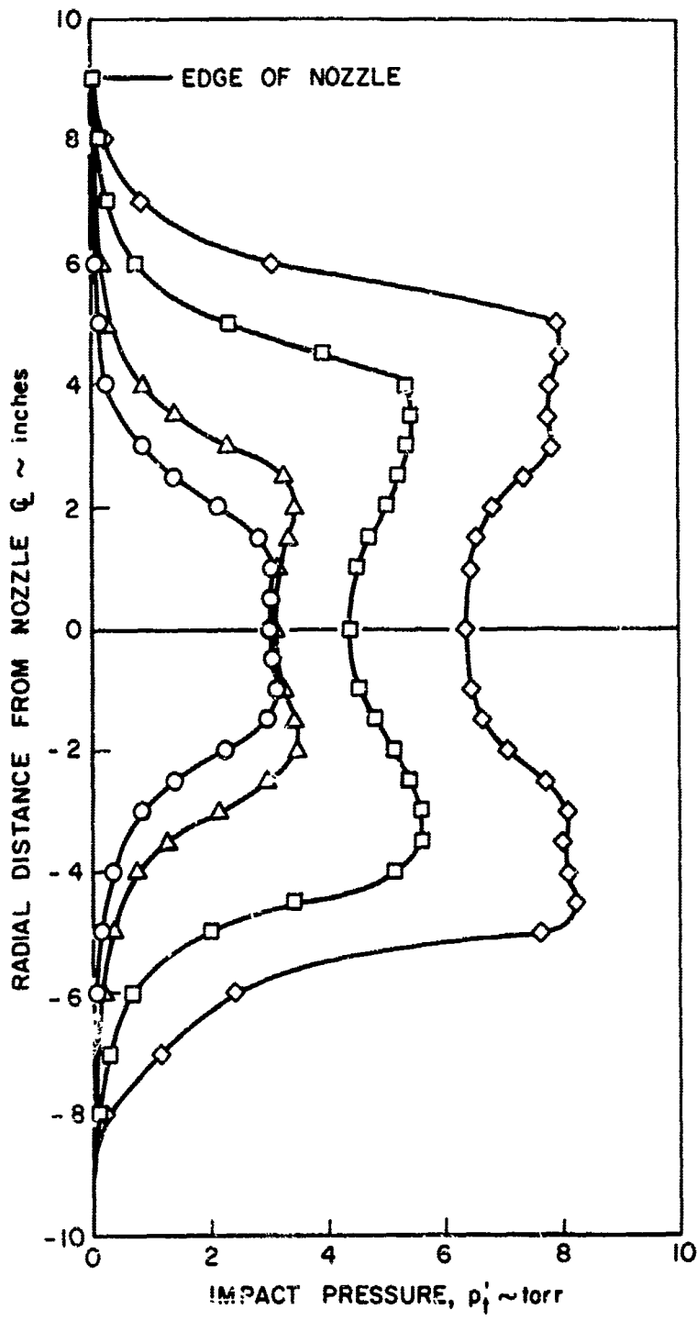

Fig. 14 Test Section Flow Conditions

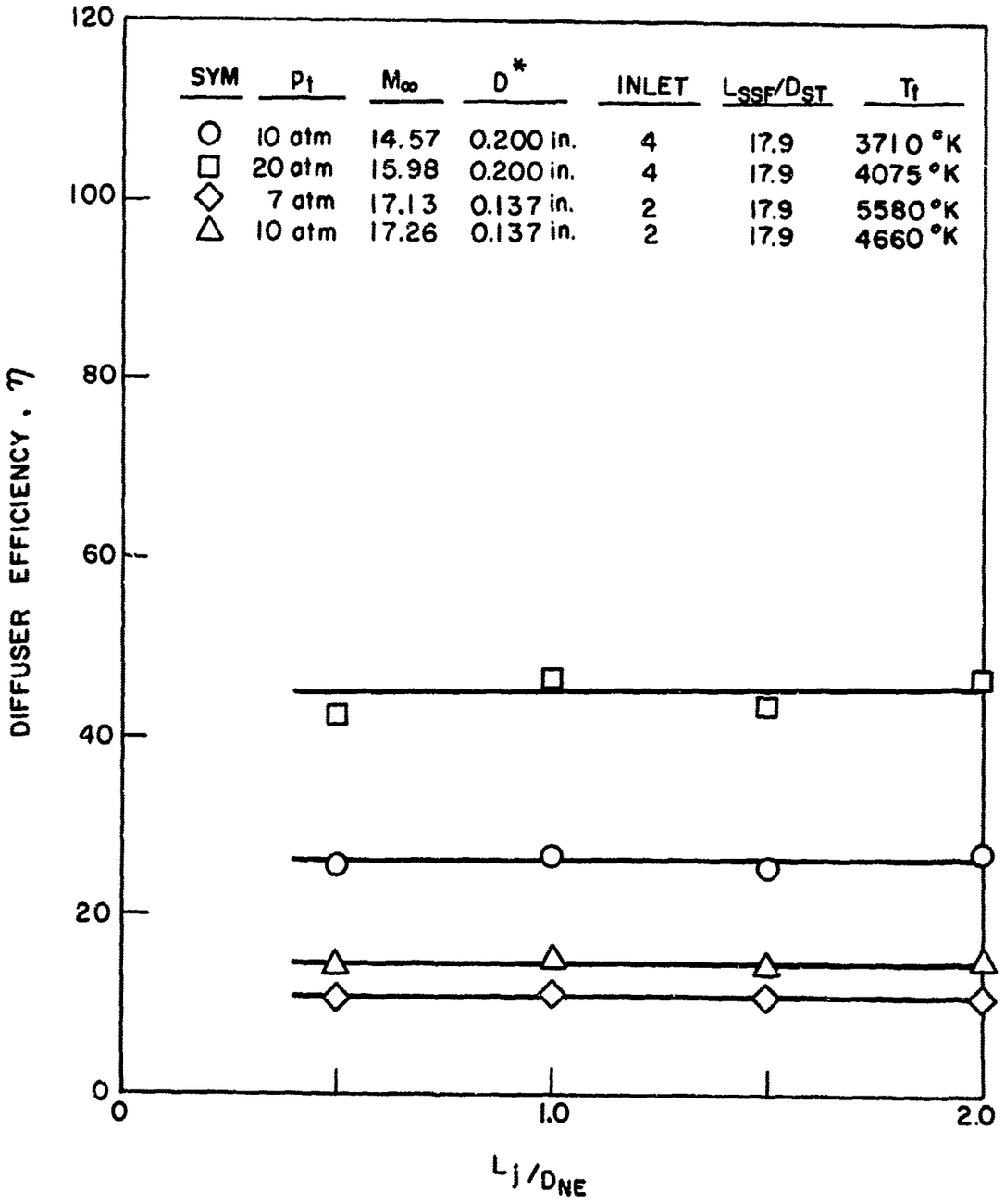

Fig. 15 Effect of Open-Jet Length on Diffuser Efficiency with Empty Test Section

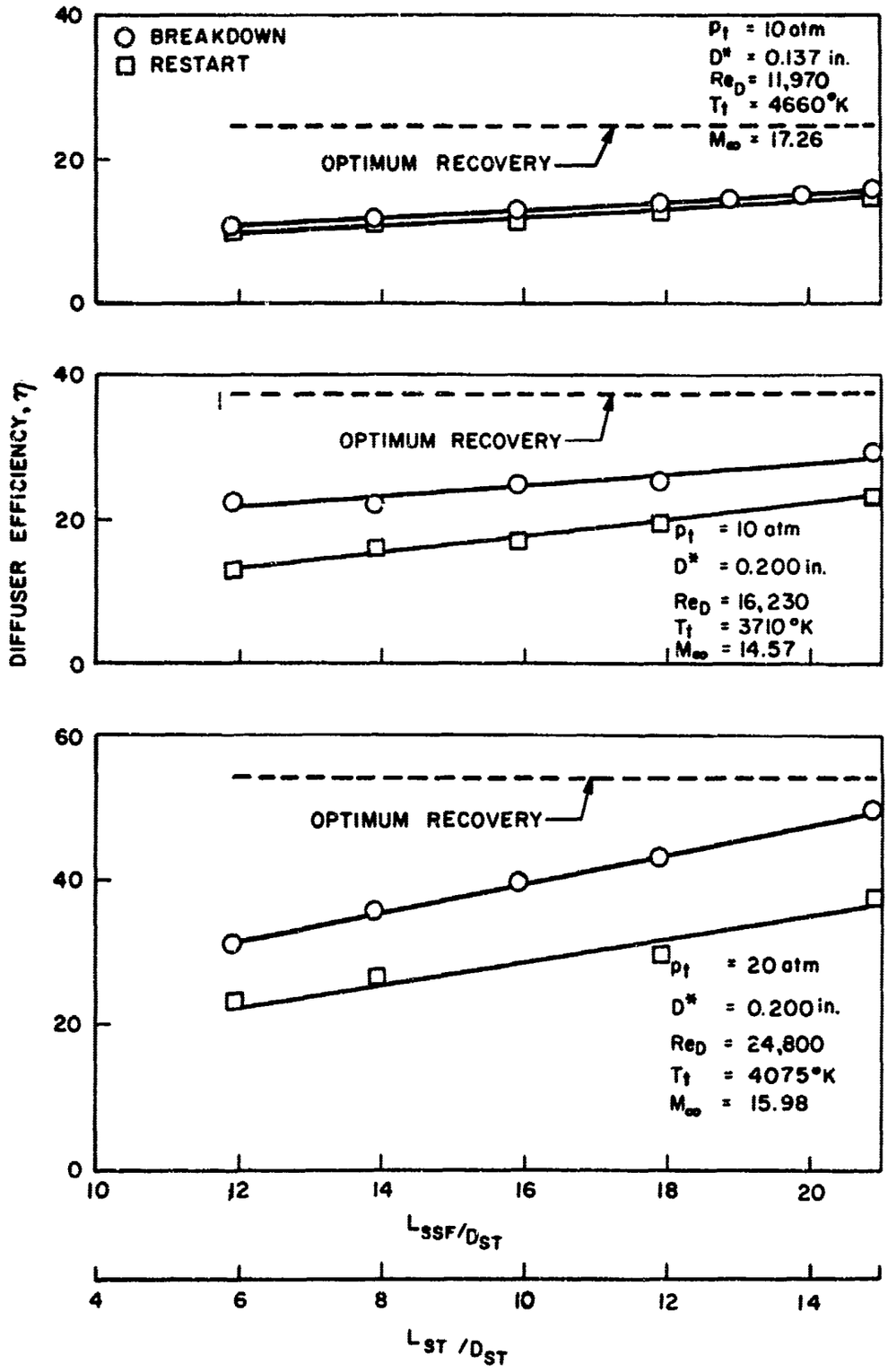

Fig. 16 Effect of Diffuser Length on Diffuser Efficiency with Empty Test Section, $L_i/D_{NE} \approx 1.5$

	p_t	D^*	Re_D	T_t	M_∞
○	10 atm	0.137 in.	11,970	4660 °K	17.26
□	10 atm	0.200 in.	16,230	3710 °K	14.57
◇	20 atm	0.200 in.	24,800	4075 °K	15.98

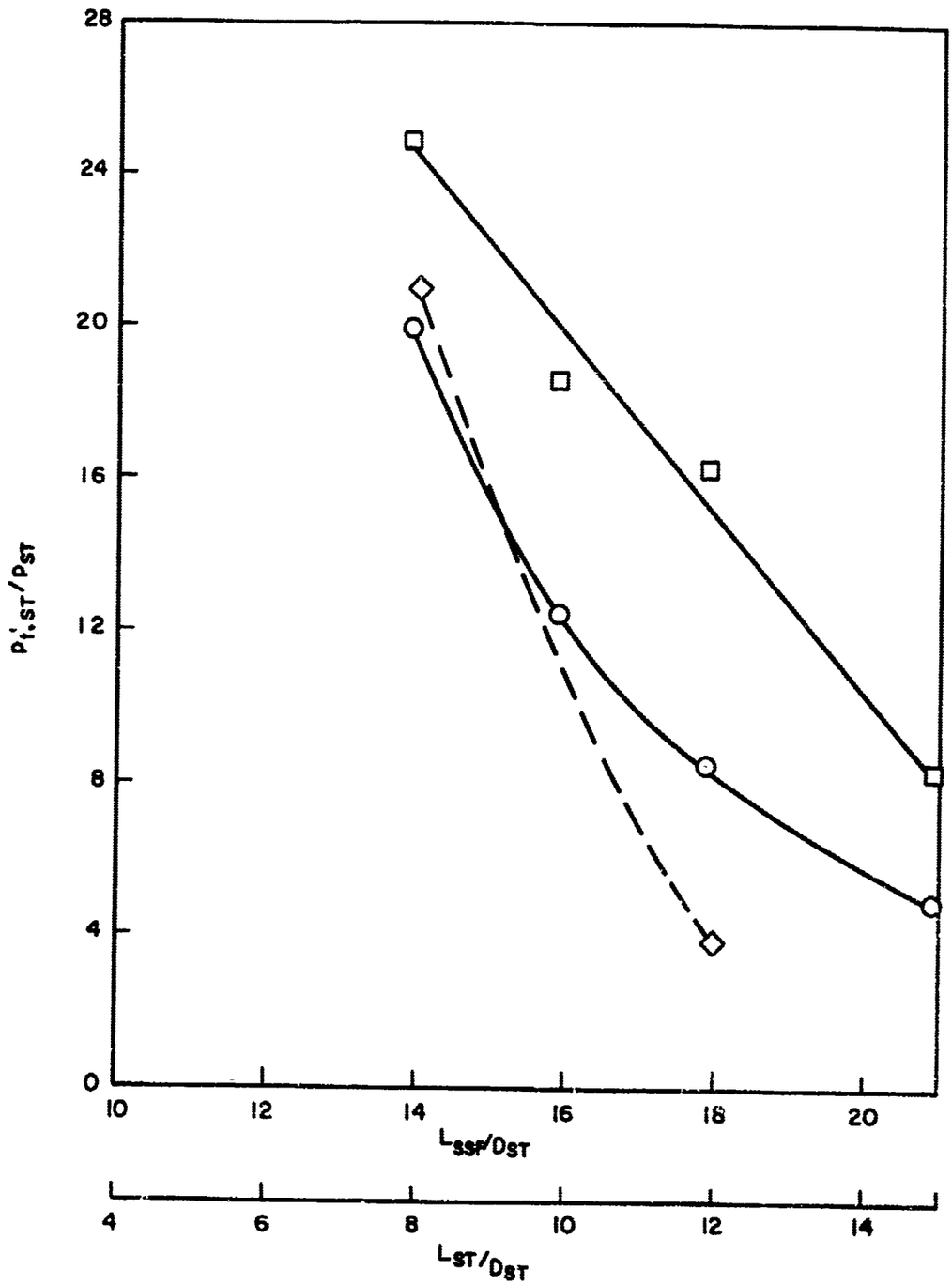

Fig. 17 Variation of Impact to Static Pressure Ratio at End of Diffuser Second Throat for Changes in Second-Throat Length with Empty Test Section, L_j/D_{NE} = 1.5

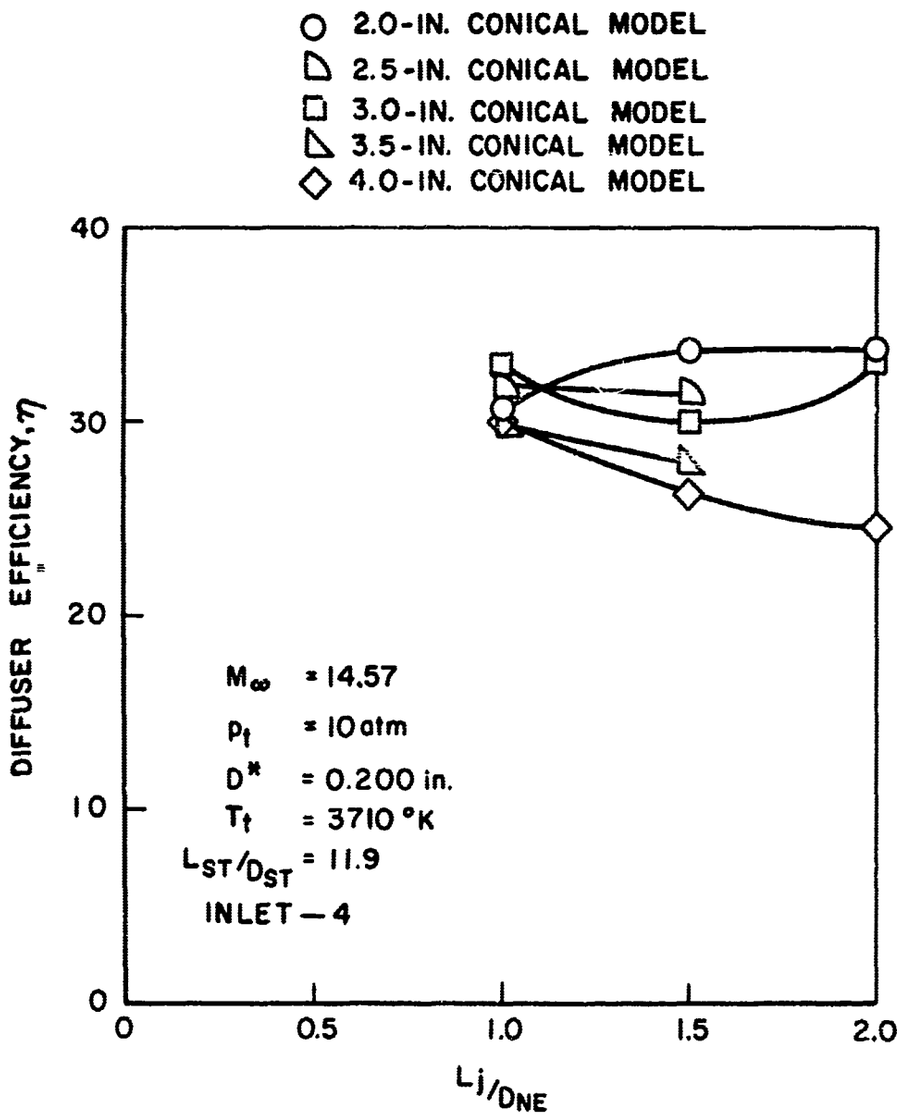

Fig. 18 Effect of Open-Jet Length on Diffuser Efficiency for Various Model Sizes

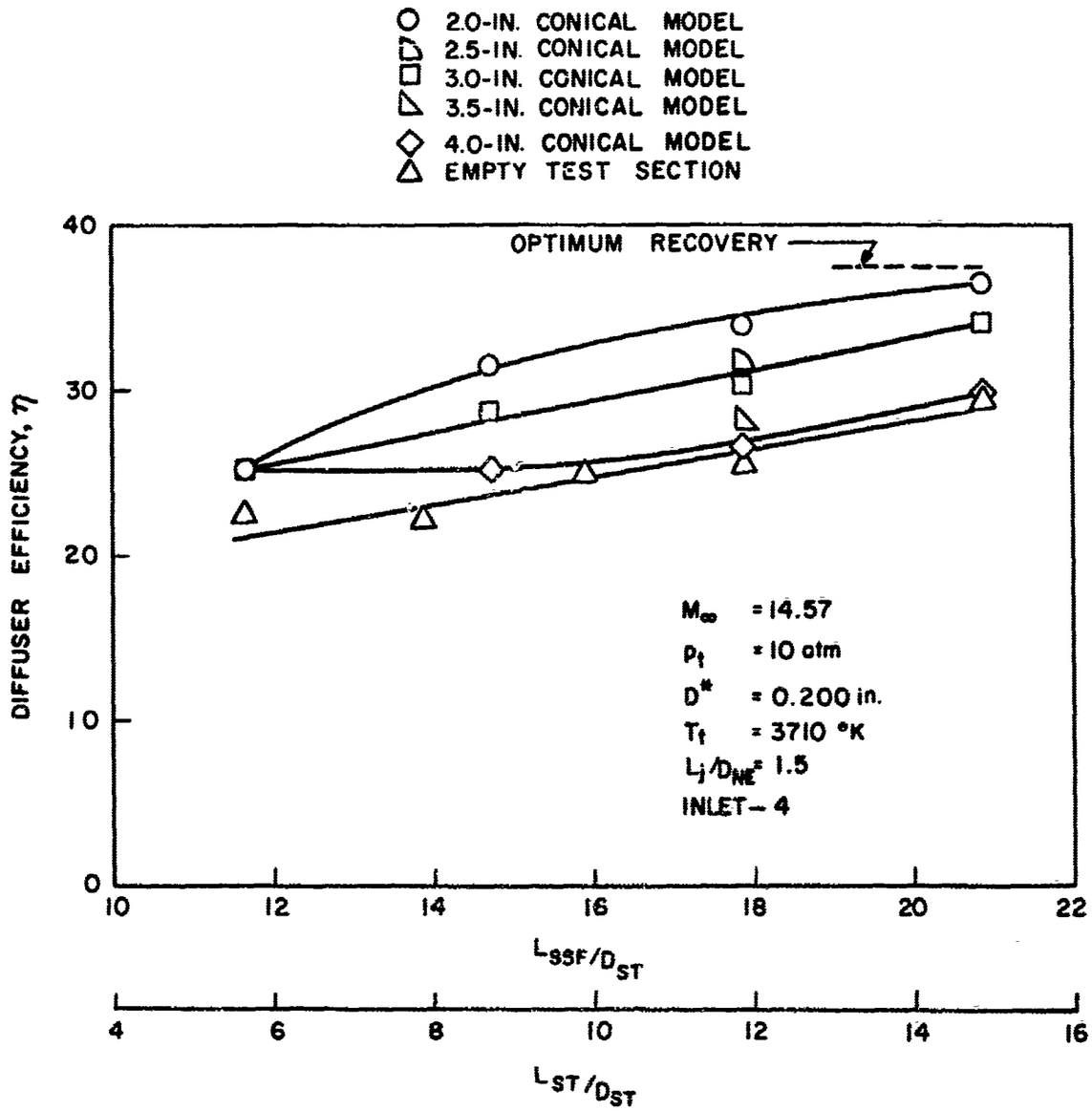

Fig. 19 Effect of Diffuser Length on Diffuser Efficiency for Various Model Sizes

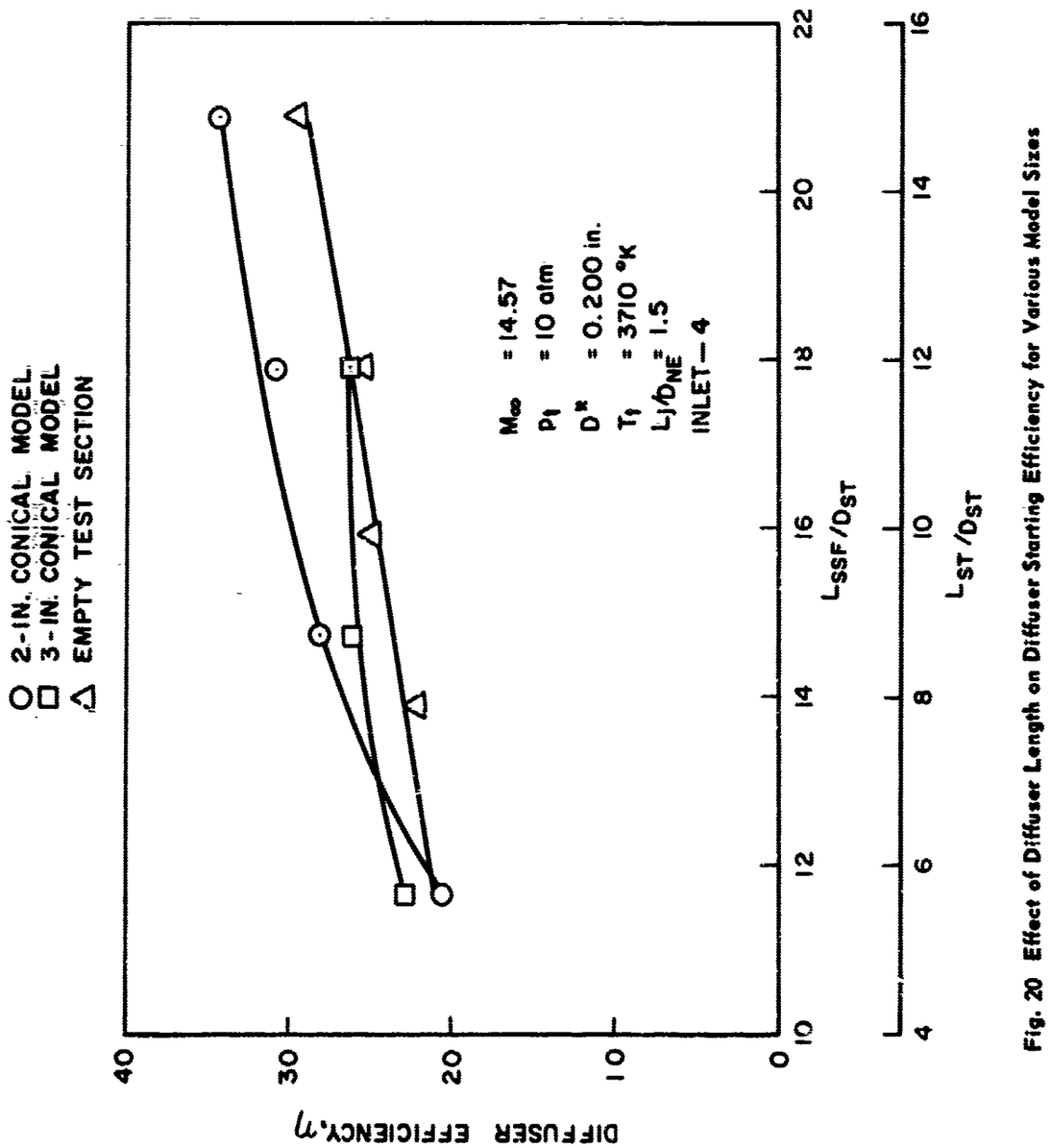

Fig. 20 Effect of Diffuser Length on Diffuser Starting Efficiency for Various Model Sizes

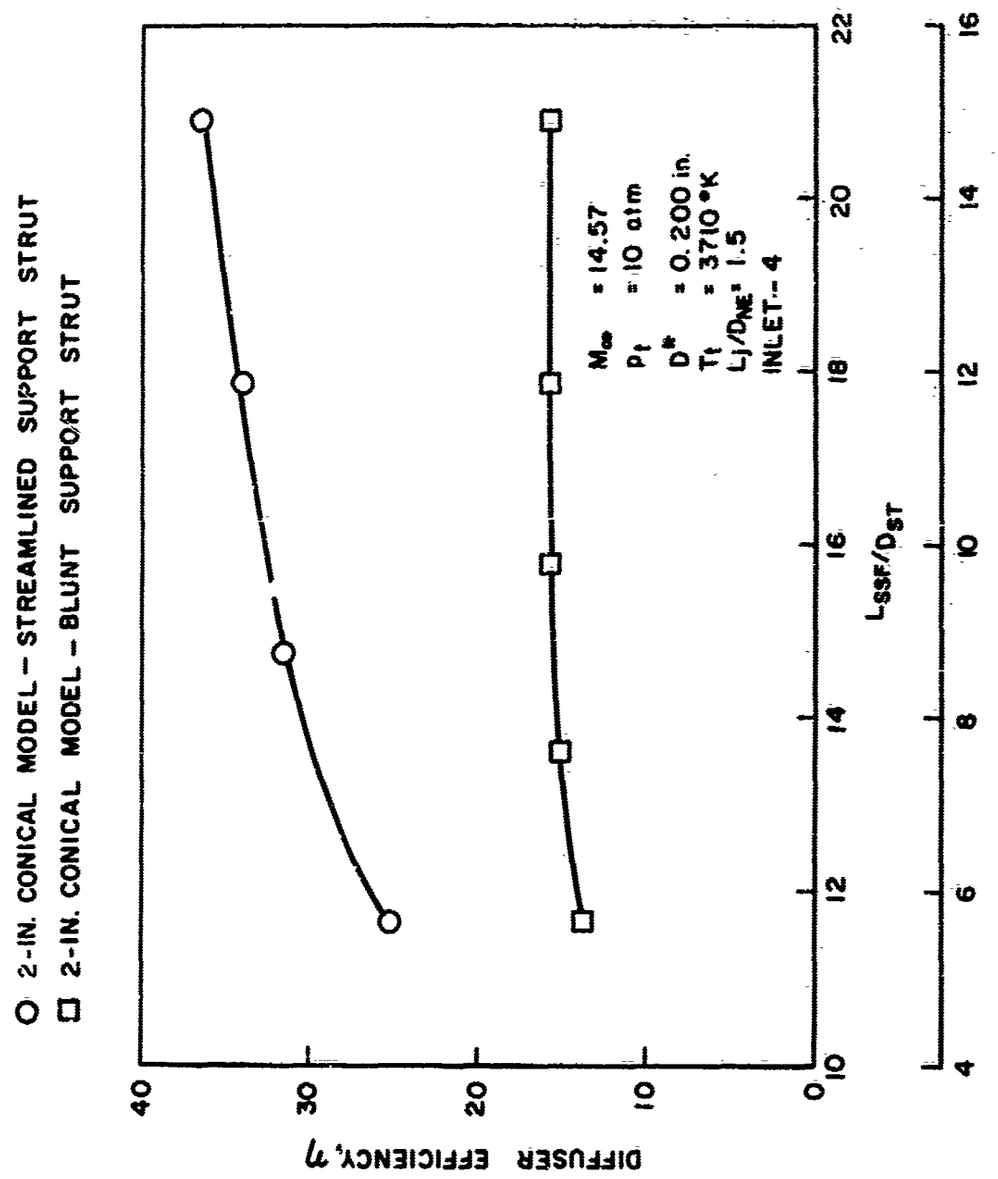

Fig. 21 Effect of Model Support Strut on Diffuser Efficiency

APPENDIX II
DERIVATION OF THE EXPRESSION FOR THE OPTIMUM DIFFUSER RECOVERY PRESSURE

Consider a one-dimensional, inviscid, hypervelocity flow stream, with cross-sectional area A_{NE}, entering a diffuser with a long constant-diameter second throat of area A_{ST}. By means of the conservation equations and the usual hypersonic approximations, the diffuser downstream pressure can be given approximately by

$$p_d \approx \left(p_{t,\infty}'\right)\left(\frac{A_{NE}}{A_{ST}}\right) \tag{II-1}$$

The only assumptions made regarding the diffusion process are that (1) the axial pressure term in the momentum equation corresponding to the diffuser inlet area change (from A_{NE} to A_{ST}) is negligible, and (2) the diffuser is sufficiently long to permit the flow to decelerate to a uniform, low-speed condition.

Extending the analysis to the condition where the flow is initially nonuniform can be done by using integrated quantities for the mass and momentum flux terms in the conservation equations. A momentum flux ratio is defined as

$$\alpha = \int_0^{A_{NE}} \left(\frac{\rho U^2\, dA}{\rho_\infty U_\infty^2 A_{NE}}\right) = \frac{\text{Area-Weighted-Average Momentum Flux}}{\text{Centerline Free-Stream Momentum Flux}} \tag{II-2}$$

The equation for diffuser pressure thus becomes

$$p_d \approx p_{t,\infty}' \,(\alpha)\left(\frac{A_{NE}}{A_{ST}}\right) \tag{II-3}$$

A second integral quality, the mass flux ratio, is also defined as

$$\beta = \int_0^{A_{NE}} \left(\frac{\rho U\, dA}{\rho_\infty U_\infty A_{NE}}\right) = \frac{\overset{\circ}{m}}{\rho_\infty U_\infty A_{NE}} = \frac{\text{Area-Weighted-Average Mass Flux}}{\text{Centerline Free-Stream Mass Flux}} \tag{II-4}$$

These two ratios, α and β, were evaluated for the test section flow properties and transverse flow variations shown in Fig. 14. The centerline flow properties were evaluated as discussed in Section 3.2.1. The variation of flow properties through the boundary layer was calculated using the

measured impact pressures and assuming a laminar (second-order polynomial) velocity profile, with the enthalpy given in terms of velocity ratio by the Crocco distribution equation. For all cases, the ratios α and β were essentially equal. Thus, one can substitute the mass flux ratio, β, into Eq. (II-3) for the quantity α. The centerline impact pressure can be related to the free-stream conditions by the hypersonic normal-shock approximation

$$P_{t,\infty}' \approx \rho_\infty U_\infty^2 \tag{II-5}$$

Substituting Eqs. (II-4) and (II-5), and the condition that $\alpha = \beta$, into Eq. (II-3) gives the final relation for the diffuser pressure as

$$P_d \approx \rho_\infty U_\infty^2 \left(\frac{\dot{m}}{\rho_\infty U_\infty A_{NE}}\right)\left(\frac{A_{NE}}{A_{ST}}\right) = \frac{\dot{m} U_\infty}{A_{ST}} \tag{II-6}$$

UNCLASSIFIED

Security Classification

DOCUMENT CONTROL DATA - R&D

(Security classification of title, body of abstract and indexing annotation must be entered when the overall report is classified)

1 ORIGINATING ACTIVITY (Corporate author) Arnold Engineering Development Center, ARO, Inc., Operating Contractor, Arnold Air Force Station, Tennessee	2a REPORT SECURITY CLASSIFICATION UNCLASSIFIED 2b GROUP N/A

3 REPORT TITLE

AN EXPERIMENTAL INVESTIGATION OF FIXED-GEOMETRY DIFFUSERS IN AN OPEN-JET WIND TUNNEL AT MACH NUMBERS BETWEEN 14 AND 18 AND REYNOLDS NUMBERS BETWEEN 8,900 AND 25,000

4 DESCRIPTIVE NOTES (Type of report and inclusive dates)

N/A

5. AUTHOR(S) (Last name, first name, initial)

White, James J., III, ARO, Inc.

6. REPORT DATE March 1967	7a TOTAL NO OF PAGES 45	7b. NO OF REFS 4
8a. CONTRACT OR GRANT NO. AF40(600)-1200 b. PROJECT NO. 7778 c. Program Element 62410034 d. Task 777805	9a ORIGINATOR'S REPORT NUMBER(S) AEDC-TR-67-3 9b. OTHER REPORT NO(S) (Any other numbers that may be assigned this report) N/A	

10. AVAILABILITY/LIMITATION NOTICES Distribution of this report is unlimited.

11. SUPPLEMENTARY NOTES Available in DDC.	12. SPONSORING MILITARY ACTIVITY Arnold Engineering Development Center, Air Force Systems Command, Arnold Air Force Station, Tennessee

13. ABSTRACT

A fixed-geometry diffuser system was tested in an arc-heated, hypersonic, open-jet wind tunnel facility at Mach numbers between 14 and 18 and Reynolds numbers (based on nozzle exit diameter) between 8,900 and 25,000. Tests were conducted both with an empty test section and with conical models in the flow. Test variables included test section open-jet length, diffuser second-throat length, and diffuser inlet geometry. Diffuser efficiency improved with increased diffuser second-throat length, with increasing Reynolds number, and with the addition of conical models into the flow. Changes in open-jet length and diffuser inlet geometry had no appreciable effect on diffuser efficiency with an empty test section. A streamlined model support strut produced marked improvement in diffuser efficiency over a blunt support strut.

DD FORM 1 JAN 64 1473

UNCLASSIFIED

Security Classification

14 KEY WORDS	LINK A		LINK B		LINK C	
	ROLE	WT	ROLE	WT	ROLE	WT
diffuser systems fixed geometry diffusers wind tunnel testing conical models tunnel-empty testing hypersonic flow						

INSTRUCTIONS

1. ORIGINATING ACTIVITY: Enter the name and address of the contractor, subcontractor, grantee, Department of Defense activity or other organization *(corporate author)* issuing the report.

2a. REPORT SECURITY CLASSIFICATION: Enter the overall security classification of the report. Indicate whether "Restricted Data" is included. Marking is to be in accordance with appropriate security regulations.

2b. GROUP: Automatic downgrading is specified in DoD Directive 5200.10 and Armed Forces Industrial Manual. Enter the group number. Also, when applicable, show that optional markings have been used for Group 3 and Group 4 as authorized.

3. REPORT TITLE: Enter the complete report title in all capital letters. Titles in all cases should be unclassified. If a meaningful title cannot be selected without classification, show title classification in all capitals in parenthesis immediately following the title.

4. DESCRIPTIVE NOTES: If appropriate, enter the type of report, e.g., interim, progress, summary, annual, or final. Give the inclusive dates when a specific reporting period is covered.

5. AUTHOR(S): Enter the name(s) of author(s) as shown on or in the report. Enter last name, first name, middle initial. If military, show rank and branch of service. The name of the principal author is an absolute minimum requirement.

6. REPORT DATE: Enter the date of the report as day, month, year; or month, year. If more than one date appears on the report, use date of publication.

7a. TOTAL NUMBER OF PAGES: The total page count should follow normal pagination procedures, i.e., enter the number of pages containing information.

7b. NUMBER OF REFERENCES: Enter the total number of references cited in the report.

8a. CONTRACT OR GRANT NUMBER: If appropriate, enter the applicable number of the contract or grant under which the report was written.

8b, 8c, & 8d. PROJECT NUMBER: Enter the appropriate military department identification, such as project number, subproject number, system numbers, task number, etc.

9a. ORIGINATOR'S REPORT NUMBER(S): Enter the official report number by which the document will be identified and controlled by the originating activity. This number must be unique to this report.

9b. OTHER REPORT NUMBER(S): If the report has been assigned any other report numbers *(either by the originator or by the sponsor)*, also enter this number(s).

10. AVAILABILITY/LIMITATION NOTICES: Enter any limitations on further dissemination of the report, other than those imposed by security classification, using standard statements such as:

(1) "Qualified requesters may obtain copies of this report from DDC."

(2) "Foreign announcement and dissemination of this report by DDC is not authorized."

(3) "U. S. Government agencies may obtain copies of this report directly from DDC. Other qualified DDC users shall request through _____."

(4) "U. S. military agencies may obtain copies of this report directly from DDC. Other qualified users shall request through _____."

(5) "All distribution of this report is controlled. Qualified DDC users shall request through _____."

If the report has been furnished to the Office of Technical Services, Department of Commerce, for sale to the public, indicate this fact and enter the price, if known.

11. SUPPLEMENTARY NOTES: Use for additional explanatory notes.

12. SPONSORING MILITARY ACTIVITY: Enter the name of the departmental project office or laboratory sponsoring *(paying for)* the research and development. Include address.

13 ABSTRACT: Enter an abstract giving a brief and factual summary of the document indicative of the report, even though it may also appear elsewhere in the body of the technical report. If additional space is required, a continuation sheet shall be attached.

It is highly desirable that the abstract of classified reports be unclassified. Each paragraph of the abstract shall end with an indication of the military security classification of the information in the paragraph, represented as *(TS), (S), (C), or (U)*.

There is no limitation on the length of the abstract. However, the suggested length is from 150 to 225 words.

14. KEY WORDS: Key words are technically meaningful terms or short phrases that characterize a report and may be used as index entries for cataloging the report. Key words must be selected so that no security classification is required. Identifiers, such as equipment model designation, trade name, military project code name, geographic location, may be used as key words but will be followed by an indication of technical context. The assignment of links, rules, and weights is optional.